Influence of Wall Contacts on Measured Complex Permittivity Spectra at Coaxial Line Frequencies

Karim E. Mattar, *Member, IEEE*, David G. Watters, *Member, IEEE*, and Morris E. Brodwin, *Life Senior Member, IEEE*

Abstract—**We examine the effects on observed complex permittivity caused by gaps between a sample and the conductors of the coaxial sample holder. A transverse resonance model relates the observed and true values given the dimensions of the gap. This model also confirms the accuracy of the simpler capacitance model for small conductivities and low frequencies. We describe how, experimentally, variation in the observed sample characteristics with frequency may be used to identify a gap problem. Experimental results demonstrate the usefulness of conducting pastes or copper plating in reducing the gap effect.**

I. Introduction

KNOWLEDGE of the frequency variation of conductivity and permittivity of solid-state electrolytes is essential for understanding the transport process in these materials [1]. It is well known that as conductivity increases errors in measurement introduced by faulty contacts between the sample and metal walls of the sample holder become increasingly serious, leading to an upper bound on measured conductivity [2]–[7]. These errors are negligible only for low-loss, low-permittivity samples. This problem has been studied for coaxial line [4], [8] and waveguide sample holders [2], [3], [5]–[9]. Prior work reported experimental results over small bandwidths. With the availability of large-bandwidth sources and network analyzers, the effect of errors caused by gaps between the material and the sample holder is now being examined over large frequency ranges. The problem became particularly apparent to us during the development of a scalar analyzer committed to materials characterization over the 2–18 GHz range [10]. Large discrepancies between measured and known material parameter values led to the analysis of the effect of gaps between the sample surface and the walls in a coaxial line sample holder over a large frequency range.

For coaxial structures with a transverse slab sample, Westphal [4] models the gap as a distributed capacitance to correct measured values. An example of results obtained with this model is shown in Fig. 1, which is a calculation of an expected observation of conductivity as a function of true conductivity for different air gap thicknesses. The dielectric constant is 12, and the frequency is 2 GHz. The presence of the gap places an upper limit on observed conductivity.

A transverse resonance model is used to correct observed data in the presence of a gap and to validate the capacitance model at low frequencies or for samples with low complex conductivities. Observed irregularities in scalar analyzer measurements identify the presence of a gap. The effect of a gap is reduced by filling the gap with conducting pastes or improving contacts by copper plating.

II. Capacitance Model

Westphal [4] treats the gap by analyzing an equivalent inhomogeneous coaxial transmission line (Fig. 2(a)), where r_i and r_o are inner and outer conductor radii, and r_{is} and r_{os} are inner and outer sample radii sample, respectively. In a homogeneous line, the inductance per unit length is $L = 1/2\pi \ln(r_o/r_i)$, and the capacitance per unit length is $C^* = 2\pi\epsilon_r^*/\ln(r_o/r_i)$, where ϵ_r^* is the complex permittivity.

When a gap of complex permittivity ϵ_{rg}^* is included (Fig. 2(b)), the *observed* capacitance is

$$C_o^* = \frac{C_{\text{gap}}^* C_{\text{samp}}^*}{C_{\text{gap}}^* + C_{\text{samp}}^*} \tag{1}$$

where $C_{\text{gap}}^* = 2\pi\epsilon_{rg}^*/L_1$, $C_{\text{samp}}^* = 2\pi\epsilon_{rs}^*/L_2$, $C_o^* = 2\pi\epsilon_{ro}^*/L_3$, and $L_2 = \ln(r_{os}/r_{is})$, $L_3 = \ln(r_o/r_i)$, and $L_1 = L_3 - L_2$.

This model neglects the junction capacitance at the boundary between the sample section and the transmission line. *Observed* sample or material permittivity, ϵ_{ro}^*, is a function of gap permittivity, ϵ_{rg}^*, and true sample permittivity, ϵ_{rs}^*:

$$\epsilon_{ro}^* = \frac{\epsilon_{rs}^* \epsilon_{rg}^* L_3}{L_1 \epsilon_{rs}^* + L_2 \epsilon_{rg}^*}. \tag{2}$$

Separating (2) into the real and imaginary parts,

$$\tan\delta_o = \frac{\epsilon_{rs} L_1 \tan\delta_g (1+\tan^2\delta_s) + \epsilon_{rg} L_2 \tan\delta_s (1+\tan^2\delta_g)}{\epsilon_{rs} L_1 (1+\tan^2\delta_s) + \epsilon_{rg} L_2 (1+\tan^2\delta_g)} \tag{3}$$

Manuscript received October 24, 1988; revised October 8, 1990. This work made use of Central Facilities supported by the National Science Foundation through the Northwestern University Material Research Center (Grant DMR 85-20280).

K. E. Mattar is with the Department of Physics, University of Calgary, Calgary, Alberta, Canada T2N 1N4.

D. G. Watters is with SRI International, Menlo Park, CA 94025.

M. E. Brodwin is with the Department of Electrical Engineering, Northwestern University, Evanston, IL 60208.

IEEE Log Number 9041944.

0018-9480/91/0300-0532$01.00 ©1991 IEEE

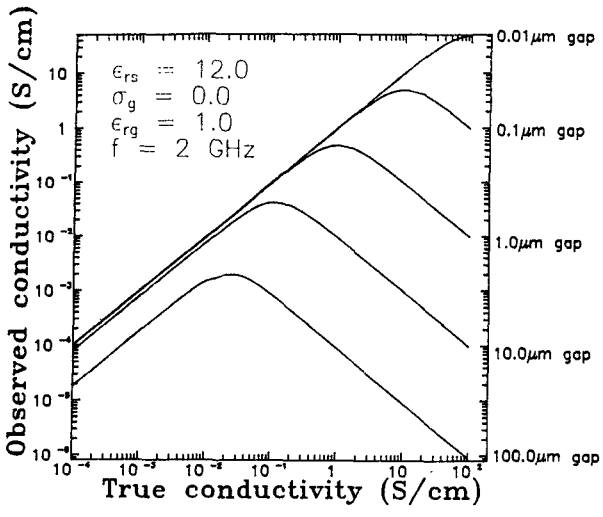

Fig. 1. Observed conductivity versus true conductivity for different gap thicknesses. It is assumed that $\epsilon_{rs} = 12.0$, $\epsilon_{rg} = 1.0$, $\sigma_g = 0.0$, $f = 2$ GHz, $r_i = 0.152$ cm, and $r_o = 0.35$ cm.

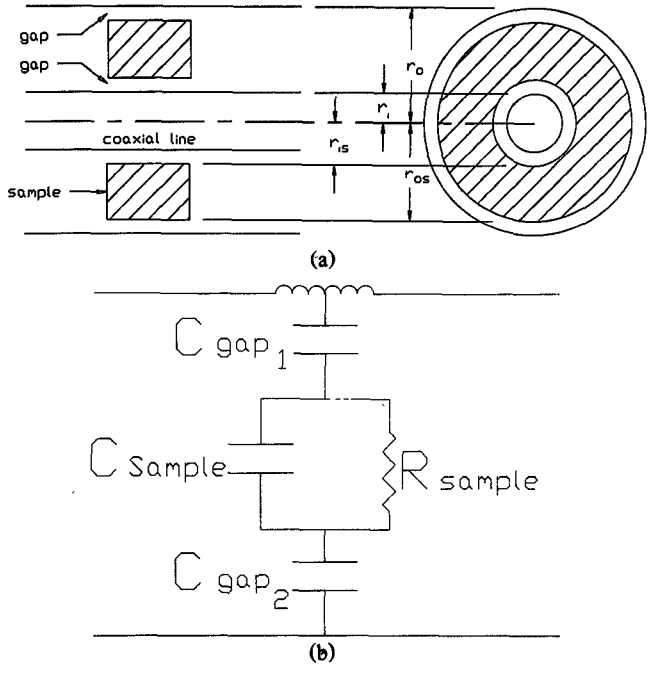

Fig. 2. (a) Schematic of a coaxial transmission line with a sample and gap region. (b) Equivalent circuit of the coaxial transmission line with a sample and lossless gap region.

and

$$\epsilon_{ro} = \epsilon_{rg}\epsilon_{rs}L_3 \cdot \frac{\epsilon_{rs}L_1(1+\tan^2\delta_s) + \epsilon_{rg}L_2(1+\tan^2\delta_g)}{(L_1\epsilon_{rs} + L_2\epsilon_{rg})^2 + (L_1\epsilon_{rs}\tan\delta_s + L_2\epsilon_{rg}\tan\delta_g)^2} \quad (4)$$

where $\tan\delta_s = \sigma_s/\omega\epsilon_o\epsilon_{rs}$, $\tan\delta_g = \sigma_g/\omega\epsilon_o\epsilon_{rg}$, and $\tan\delta_o = \sigma_o/\omega\epsilon_o\epsilon_{ro}$.

The observed conductivity, σ_o, is shown in Fig. 1 as a function of σ_s to illustrate the effect of the gap. A gap as small as 0.01 μm produces erroneous measurements for

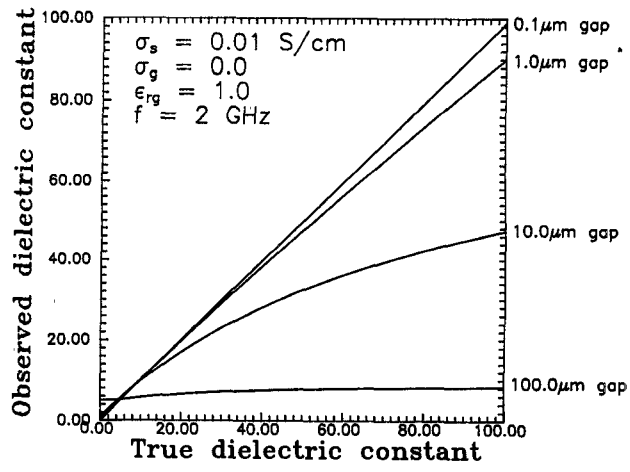

Fig. 3. Observed dielectric constant versus true dielectric constant for different gap thicknesses. It is assumed that $\sigma_s = 0.01$ S/cm, $\epsilon_{rg} = 1.0$, $\sigma_g = 0.0$, $f = 2$ GHz, $r_i = 0.152$ cm, and $r_o = 0.35$ cm.

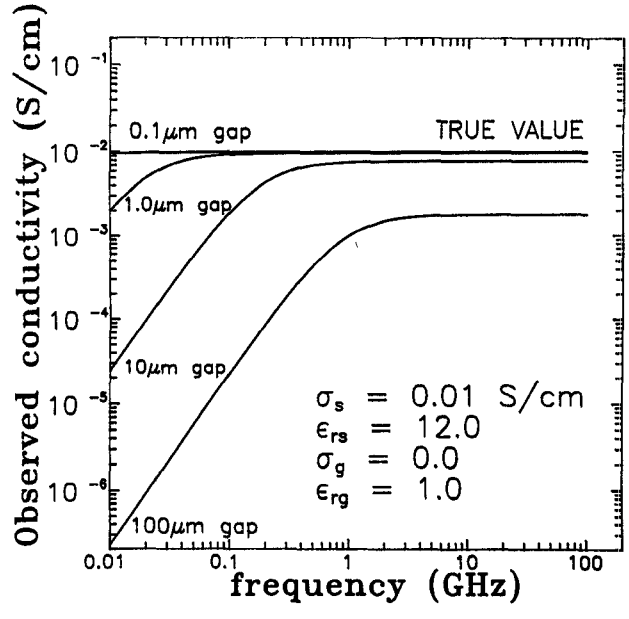

Fig. 4. Observed conductivity versus frequency for different gap thicknesses. It is assumed that $\sigma_s = 0.01$ S/cm, $\epsilon_{rg} = 12.0$, $\epsilon_{rg} = 1.0$, $\sigma_g = 0.0$, $r_i = 0.152$ cm, and $r_o = 0.35$ cm.

conductivities greater than 100 S/cm. Similarly, ϵ_{ro} is plotted in Fig. 3 as a function of ϵ_{rs}. The presence of a gap places a limit upon observed dielectric constant:

$$\lim_{\epsilon_{rs}\to\infty} \epsilon_{ro} = \epsilon_{rg}\frac{L_3}{L_1}. \quad (5)$$

Using (3), the spectral response of observed conductivity was calculated and plotted in Fig. 4 for a true conductivity of 0.01 S/cm and a true dielectric constant of 12. The figure shows the spectral response of observed conductivity for air gaps of 0.1, 1.0, 10, and 100 μm. Except for the 0.1 μm air gap, as frequency increases, so does observed conductivity. Even the maximum value for observed conductivity is not the the value.

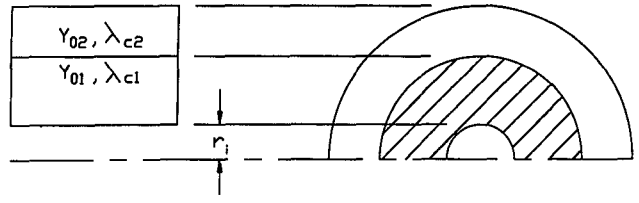

Fig. 5. Cross-sectional view of the sample region in the presence of an outer gap, and its equivalent network parameters.

III. Transverse Resonance Model of the Inhomogeneous Coaxial Line

Marcuvitz [11] presents a transverse resonance analysis of a coaxial line with a lossy dielectric which provides a more accurate analysis of the gap–sample geometry. This model views the cross section of the partially filled coaxial line as a radial transmission line, and the propagation constant for the dominant mode in the inhomogeneous coaxial line is to be determined. A single gap between sample and outer conductor simplifies the analysis. From a reference plane at the boundary between the sample and the gap, an equivalent network of two short-circuited radial transmission lines of different characteristic admittance, Y_{01} and Y_{02}, is assumed (Fig. 5). The method of transverse resonance states that the system will propagate when it is resonant in the transverse plane or, equivalently, when the admittances are equal at the gap–sample boundary [11, eq. (1)], viz.,

$$Y_{01}\,\mathrm{ct}[k_{c1}r_{os}, k_{c1}r_i] = Y_{02}\,\mathrm{ct}[k_{c2}r_{os}, k_{c2}r_o] \tag{6}$$

where

$$\frac{Y_{02}}{Y_{01}} = \frac{k_{c1}\epsilon^*_{rg}}{k_{c2}\epsilon^*_{rs}} \tag{7}$$

and the sample and gap permittivities are in general complex, k_{c1}, and k_{c2} are the wave numbers in each region, and $\mathrm{ct}(x, y)$ is the radial cotangent. In the general case, both the sample and the gap are lossy; consequently, the radial cotangent functions are complex. The usual separation relations apply:

$$k_{c1}^2 - \gamma^2 = \frac{\omega^2}{c^2}\epsilon^*_{rs} \tag{8}$$

and

$$k_{c2}^2 - \gamma^2 = \frac{\omega^2}{c^2}\epsilon^*_{rg} \tag{9}$$

where γ is the propagation constant of the region, $\gamma = j(\omega/c)\sqrt{\epsilon^*_{ro}}$. Solving for ϵ^*_{ro} from (6)–(9), we have

$$\epsilon^*_{ro} = \epsilon^*_{rs}\epsilon^*_{rg}\frac{\left(\epsilon^*_{rg}(\mathrm{ct})^2[k_{c2}r_{os}, k_{c2}r_o] - \epsilon^*_{rs}(\mathrm{ct})^2[k_{c1}r_{os}, k_{c1}r_i]\right)}{\epsilon^{*2}_{rg}(\mathrm{ct})^2[k_{c2}r_{os}, k_{c2}r_o] - \epsilon^{*2}_{rs}(\mathrm{ct})^2[k_{c1}r_{os}, k_{c1}r_i]}. \tag{10}$$

Since the arguments of the radial cotangents are functions of ϵ^*_{ro}, (10) is transcendental and is solved by iteration.

Marcuvitz presents an approximate solution in the low frequency range: $k_{c1}r_{os} < 1$ and $k_{c2}r_o < 1$. Here (10) reduces to

$$\epsilon_{ro} \approx \epsilon_{rs}\epsilon_{rg}\frac{\ln\left(\frac{r_o}{r_i}\right)}{\epsilon_{rs}\ln\left(\frac{r_o}{r_{os}}\right) + \epsilon_{rg}\ln\left(\frac{r_{os}}{r_i}\right)}. \tag{11}$$

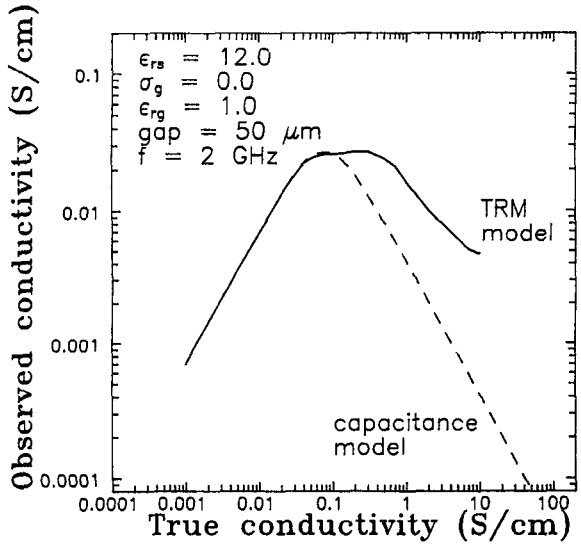

Fig. 6. Observed conductivity versus true conductivity for the transverse resonance model. It is assumed that $\epsilon_{rs} = 12.0$, $\epsilon_{rg} = 1.0$, $\sigma_g = 0.0$, $f = 2$ GHz, $r_i = 0.152$ cm, $r_o = 0.35$ cm, and outer gap = 50 μm.

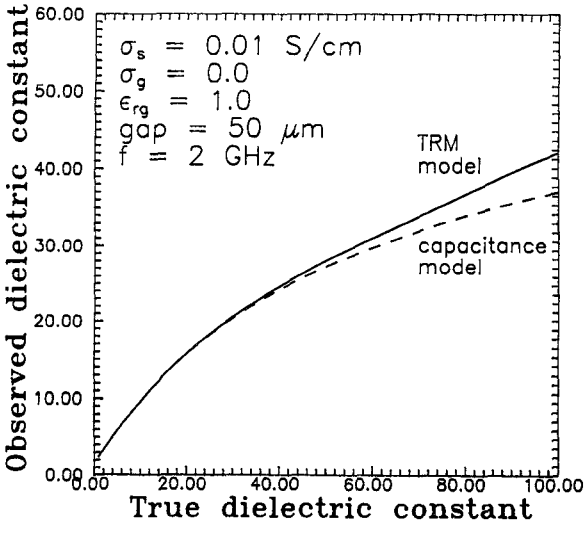

Fig. 7. Observed dielectric constant versus true dielectric constant for the transverse resonance model. It is assumed that $\sigma_s = 0.01$ S/cm, $\epsilon_{rg} = 1.0$, $\sigma_g = 0.0$, $f = 2$ GHz, $r_i = 0.152$ cm, $r_o = 0.35$ cm, and outer gap = 50 μm.

Thus, in the low frequency limit, the transverse resonance result reduces to the capacitance model when the model is developed for a single gap (where r_{ri} is set equal to r_i) in (2).

We next compare both models by calculating an observed conductivity and dielectric constant for an outer gap of 50 μm and a true dielectric constant of 12. Fig. 6 shows observed conductivity as a function of true conductivity, obtained using (10). The dashed curve represents the capacitance model, and the solid curve represents the transverse resonance model. Both models coincide to a maximum and then deviate for greater true conductivity. Fig. 7 shows observed dielectric constant as a function of true dielectric constant for a true conductivity of 0.01 S/cm.

The transverse resonance model establishes the range of validity of the capacitance model. For example, the simpler model is valid up to the peak in the true conductivity curve

in Fig. 6. The capacitance model is also valid of the smaller values for low true dielectric constant (Fig. 7). If the gap dimensions were known, either by observation or by calculation of differential expansion arising from an extended temperature range [13], then the true values of conductivity and dielectric constant could be determined by using the transverse resonance model. Solving for ϵ_{rs}^* from (6)–(9), we have

$$\epsilon_{rs}^* = -\frac{b}{2} \pm \sqrt{\left(\frac{b}{2}\right)^2 - \epsilon_{ro}^* \cdot b} \tag{12}$$

where

$$b = \frac{\epsilon_{rg}^{*2}(\mathrm{ct})^2[k_{c2}r_{os}, k_{c2}r_o]}{(\mathrm{ct})^2[k_{c1}r_{os}, k_{c1}r_i](\epsilon_{ro}^* - \epsilon_{rg}^*)}. \tag{13}$$

If sample parameters are within the range of validity of the capacitance model, then ϵ_{rs}^* for a two-gap model is (from (2))

$$\epsilon_{rs}^* = \frac{\epsilon_{ro}^* \epsilon_{rg}^* L_2}{\epsilon_{rg}^* L_3 - \epsilon_{ro}^* L_1}. \tag{14}$$

Thus, with a knowledge of the dimensions and composition of the gap material, together with the observed dielectric constant and conductivity, the true characteristics of the sample can be determined.

IV. Eliminating Gap Effects

In general, it is difficult to determine the size of the gap, and thus we seek ways of reducing or eliminating the effect of the gap. The capacitance model indicates that the gap effect is reduced by increasing gap capacitance so that it is much larger than sample capacitance. This is accomplished by filling the gap with high-dielectric-constant material. Equations (3) and (4) are greatly simplified assuming $\epsilon_{rs}L_1 \ll \epsilon_{rg}L_2$, and $L_3 \approx L_2$.

There are two ways of forcing the observed values to approximate the true values. One way is to note that when $\tan^2\delta_s \ll 1$ and $\tan^2\delta_g \ll 1$, the desired result for ϵ_r can be obtained. These inequalities are equivalent to stating that the method is valid only for low-loss materials. The interim result for $\tan\delta$ is

$$\tan\delta_o \approx \tan\delta_s + \tan\delta_g \frac{\epsilon_{rs}L_1}{\epsilon_{rg}L_2}. \tag{15}$$

$\tan\delta_s$ will be equal to $\tan\delta_o$ if $\epsilon_{rs}L_1\tan\delta_g \ll \epsilon_{rg}L_2\tan\delta_s$. Since $\epsilon_{rs}L_1 \ll \epsilon_{rg}L_2$, from the small-gap approximation, this inequality is easily satisfied.

This result agrees with the well-known approximation that small air gaps can be neglected for low-loss materials. It extends this idea by showing that filling the gap with a high-dielectric-constant material expands the range of gap widths which can be tolerated. For example if ϵ_{rg} is large, the small-gap approximation can be satisfied for larger gaps. And if $\tan\delta_g$ and ϵ_{rg} still satisfy $\epsilon_{rs}L_1\tan\delta_g \ll \epsilon_{rg}L_2\tan\delta_s$, the observed values equal the true values.

Another way of forcing the observed values to approximate the true values is filling the gap with a highly conducting material, and thus approach the limit of a perfect fit. If we assume small gaps ($\epsilon_{rs}L_1 \ll \epsilon_{rg}L_2$, and $L_2 \approx L_3$), and $\tan\delta_g \geqslant \tan\delta_s$, then observed values will approach true values. This result is established by using these assumptions in (3) and (4) and using the small-gap approximation to obtain

$$\tan\delta_o \approx \tan\delta_s + \tan\delta_g \frac{\epsilon_{rs}L_1}{\epsilon_{rg}L_2\left(1+\tan\delta_g^2\right)} \tag{16}$$

and

$$\epsilon_{ro} \approx \frac{\epsilon_{rs}L_3}{L_2} \approx \epsilon_{rs}. \tag{17}$$

If it is additionally assumed that the loss tangent of the sample is greater than or equal to 1, then the observed loss tangent is approximately equal to the loss tangent of the sample.

V. Experimental Investigation

We now describe experiments for mitigating the gap effect for lossy samples. The theoretical discussion indicates that the gap effect is reduced if the gap is small, and if it contains a material with loss tangent greater than or equal to the loss tangent of the sample. Thus the conductivity of the filling limits the highest measurable sample conductivity.

Two techniques were used to fill the gap. The first employed a silver conducting paste, 5450 Thermoplastic.[1] The paste was painted on the curved surfaces of the sample, the sample was inserted into the sample holder, and excess paste was removed. The second technique is to electroplate a rigid sample. The process requires four steps [14]. 1) Solutions of nitric and hydrofluoric acid are used to clean the sample. 2) A sulfuric acid and potassium dichromate solution prepares the surface of the sample to receive an adherent metallic film for carrying the current necessary for subsequent electroplating. 3) An ammonium hydroxide based silvering solution and a formaldehyde-based reducing solution chemically deposit the silver film. 4) The sample is electroplated with copper. The flat surfaces are sanded to remove the copper and silver, and the curved surfaces are sanded for a snug fit.

The characteristics of three known samples of varying conductivities were measured using a scalar network analyzer method [10]. Measurements were made on Stycast HiK[2] and on two silicon samples at room temperature. In each case, an APC-7 connector was used as the sample holder. Fig. 8 is a graph of the magnitude of the reflection coefficient versus frequency for a 4.43-mm-thick Stycast HiK sample. The stated dielectric constant of the sample is 16. The crossed points joined by a dashed curve represent measurements of the sample with an air gap. This curve has large irregularities, which are attributed to the simulation of higher order modes in the air gap. The half-wavelength resonant point gives an erroneous dielectric constant estimate of 10.4. From the capacitance model, an air gap of 10 μm would cause this shift in dielectric constant. The circled points represent measurements of the sample with the gap filled with the conducting paste. The half- and one-wavelength resonant point gives a dielectric constant estimate of 15.9. The solid line represents theoretical magnitude of reflection coefficient of the known sample, assuming zero gap, a dielectric constant of 16, and a conductivity of 0.005 S/cm. This

[1] 5450 Thermoplastic is a silver polymer conducting paste made by Cermalloy Inc., Union Hill Industrial Park, West Conshocken, PA 19428.

[2] Stycast HiK is a product of Emerson & Cumming, Inc.

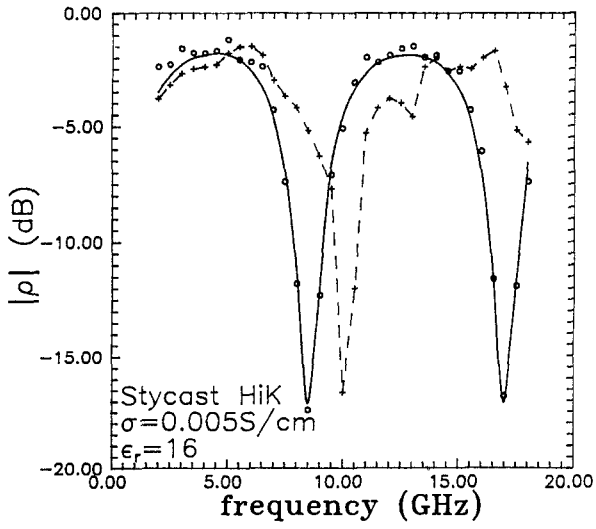

Fig. 8. $|\rho|$ versus frequency for the Stycast HiK $\epsilon_r = 16$ material. The crossed points connected by a dashed curve represent the experimental results with an air gap. The circled dots are the experimental results with the filled gap, and the solid line is the theoretical curve based on $\sigma = 0.005$ S/cm.

conductivity was chosen for best fit of the theoretical resonance curve to the experimental data.

An evaluation of the effectiveness of copper plating for a sample of p-type, (111) oriented, single-crystal silicon is considered. Measurements of the sample at dc, using the four-point probe method [15], showed a dc conductivity of 0.017 S/cm. Silicon has a published permittivity of 11.8 in the microwave range [16]. Parts (a) and (b) of Fig. 9 are graphs of the magnitude of the measured reflection and transmission coefficients as a function of frequency for the 4.50 mm sample. Measurements of reflection with the air gap (dashed curve) are again characterized by comparatively large irregularities and a shifted resonant point. Measurements of the magnitude of the reflection coefficient of the copper-plated sample produced a half-wavelength resonant point from which a dielectric constant estimate of 11.6 was obtained. In addition, by theoretically fitting the resonance curve to the experimental one (solid line), an approximate conductivity of 0.02 S/cm is calculated. Fig. 9(b) shows that the magnitude of the transmission coefficient for the sample with the air gap (dashed curve) is greater than that of the copper-plated sample (circled points).

Lastly, we evaluate the effectiveness of a copper-filled gap for a high-loss p-type, (111) oriented silicon sample. Measurements at dc gave a conductivity of $0.28 \pm 10\%$ S/cm. Fig. 10 is a graph of the transmission coefficient as a function of frequency for a 3.60 mm sample. A thinner sample is chosen to increase transmission through the lossy material. Measurements of the copper-plated sample are compared with theoretical curves for conductivities of 0.2, 0.25, and 0.3 S/cm and an assumed dielectric constant of 11.8. The transmission coefficient agrees at low frequencies with the 0.2 S/cm theoretical curve and at high frequencies with the 0.25 S/cm curve. The discrepancy between dc conductivity and measured microwave conductivity is attributed to imperfect contact between the copper plating and the sample holder. Imperfect contact was detected by placing candle soot on the copper plating, inserting and removing the sample from the sample holder, and noticing that some soot

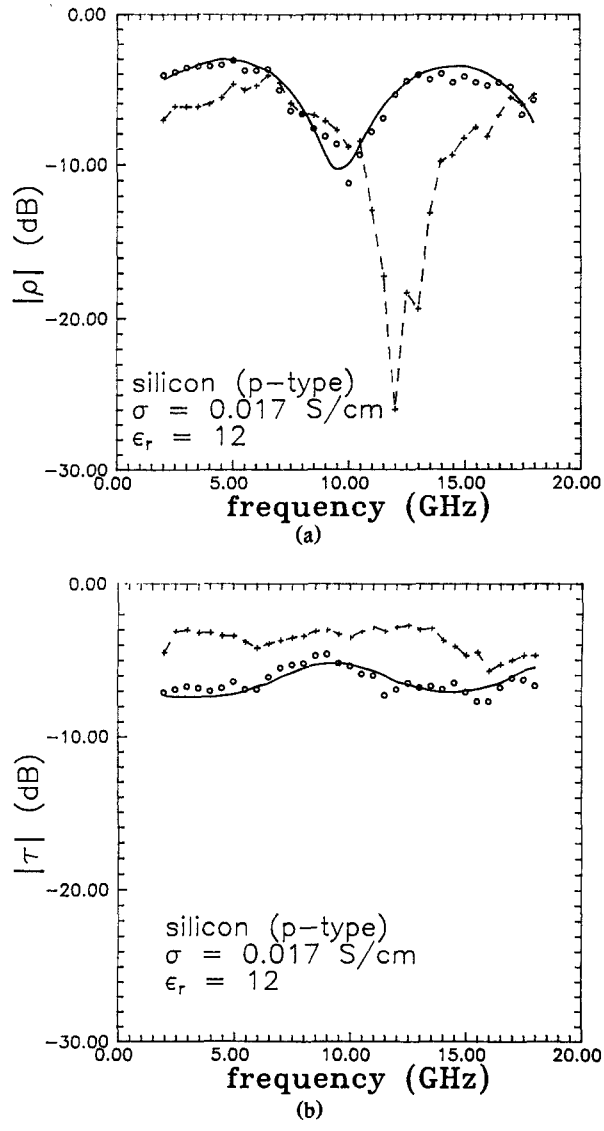

Fig. 9. (a) $|\rho|$ versus frequency for the p-type silicon sample. The crossed points connected by a dashed curve represent the experimental results with an air gap. The circled dots are the experimental results with the filled gap, and the solid line is the theoretical curve based on $\sigma = 0.017$ S/cm and $\epsilon_r = 12$. (b) $|\tau|$ versus frequency for the p-type $\sigma = 0.017$ S/cm and $\epsilon_r = 12$ silicon sample. The crossed points connected by a dashed curve represent the experimental results with an air gap. The circled dots are the experimental results with the filled gap, and the solid line is the theoretical curve.

remained on the plating. The magnitude of the reflection coefficient is not shown because it was too small and produced no resonant curves for characterizing samples accurately with the scalar network analyzer [10].

These results confirm the usefulness of the gap-filling technique. Furthermore, they demonstrate the effectiveness of using conducting paste or electroplating to reduce the gap effect.

VI. Conclusion

A gap between a sample and the conducting walls of its holder can severely limit accurate microwave material characterization. There are several ways of modeling the gap. One of the simplest is the capacitance model. According to this model, if the square of the loss tangent of the sample is

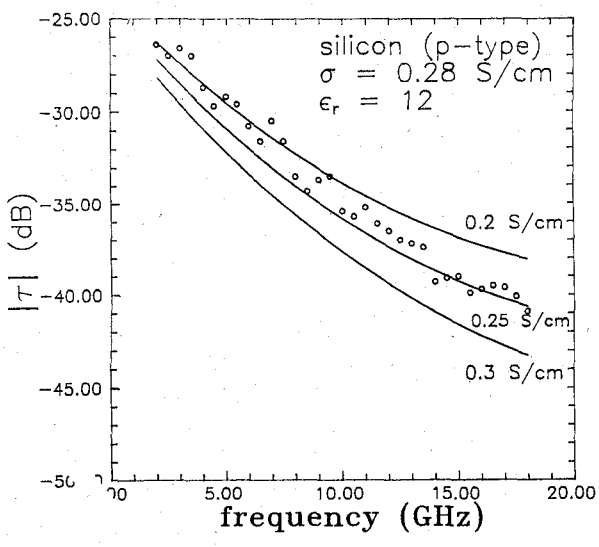

Fig. 10. $|\tau|$ versus frequency for the p-type $\sigma = 0.28$ S/cm ± 10 circled dots are the experimental results with the filled gap.

less than 1 and if the air gap is small ($\epsilon_{rs} L_1 \ll \epsilon_{rg} L_2$), the gap does not introduce significant errors. Fig. 1 demonstrates that the severity of the gap effect increases as sample loss tangent increases. Scalar analyzer measurements identify a gap problem by observing large irregularities in the data as a function of frequency when a gap is present. In a coaxial transmission-line sample holder, the only solution to the gap problem for wide-band measurements of solid samples is to fill the gap with a conducting material. The capacitance model also shows that the highest measurable conductivity is limited by the conductivity of the gap material. The error becomes larger as the conductivity of the sample exceeds the conductivity of gap material. The gap can be filled by using a conducting paste for lower-conductivity samples or by plating for higher-conductivity samples.

References

[1] T. Wong, M. E. Brodwin, D. F. Shriver, and J. I. McOmber, "Ionic conduction and dielectric relaxation of the superionic conductor Ag_2HgI_4," *Solid State Ionics*, nos. 3 and 4, p. 53, Aug. 1981.

[2] J. R. Dygas, "Study of electric properties and structure of nascicon-type solid electrolytes," Ph.D dissertation, Northwestern University, 1986.

[3] K. S. Champlin and G. H. Glover, "'Gap effects' in measurement of large permittivities," *IEEE Trans. Microwave Theory Tech.*, vol. MTT-14, pp. 397–398, Aug. 1966.

[4] W. B. Westphal, "Techniques for measuring the permittivity and permeability of liquids and solids in the frequency range 3c/s to 50kmc/s," Tech. Report XXXVI, Lab. for Insulation Research, MIT, July 1950.

[5] K. S. Champlin, J. D. Holm, and G. H. Glover, "Electrodeless determination of semiconductor conductivity from TE_{01}-mode reflectivity," *J. Appl. Phys.*, vol. 38, no. 1, pp. 96–98, Jan. 1967.

[6] K. S. Champlin and G. H. Glover, "Influence of waveguide contact in measured complex permittivity of semiconductor," *J. Appl. Phys.*, vol. 37, no. 6, pp. 2355–2360, Mar. 1966.

[7] J. Dygas and M. E. Brodwin, "Frequency-dependent conductivity of nasicon ceramics in the microwave region," *Solid State Ionics*, nos. 18 and 19, pp. 981–986, 1986.

[8] H. E. Bussy and I. E. Gray, "Measurement and standardization of dielectric samples," *IRE Trans. Instrum.*, pp. 162–165, Dec. 1963.

[9] S. B. Wilson, "Modal analysis of the 'gap effect' in waveguide dielectric measurements," *IEEE Trans. Microwave Theory Tech.*, vol. 36, p. 752, Apr. 1988.

[10] D. Watters and M. E. Brodwin, "Automatic material characterization at microwave frequencies," *IEEE Trans. Instrum. Meas.*, vol. 32, pp. 280–284, June 1988.

[11] N. Marcuvitz, *Waveguide Handbook*, (MIT Rad Lab Series, vol. 10). New York: McGraw-Hill, 1948, p. 396.

[12] K. E. Mattar, "Wide-band electromagnetic characterization of ionic and superconductors," Ph.D. dissertation, Northwestern University, 1988.

[13] E. Kuster, D. Acree, and R. L. Moore, "A calculation of measurement errors arising from air gaps in dielectric/magnetic reflectometer measurements," presented at URSI Radio Science meeting, Syracuse, NY, June 6–10, 1988.

[14] H. Narcus, *Metallizing of Plastics*. New York: Reinhold, 1960.

[15] Annual Book of ASTM Standards, Part 43, p. 404, 1978.

[16] M. Moreno, *Microwave transmission design*. New York: McGraw-Hill, 1948.

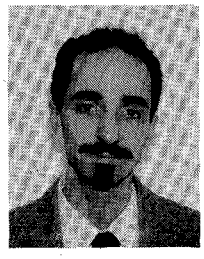

Karim E. Mattar (S'86–M'88) was born on March 28, 1957. He received the B.S. degree from Georgetown University, Washington, DC, the M.S. degree from the University of Michigan, Ann Arbor, and the Ph.D. degree from Northwestern University in November 1989.

He is currently a post-doctoral fellow in the Department of Physics, University of Calgary, Calgary, Canada. His current research includes the design and development of microwave systems for characterizing liquids and measuring oil films on water.

David G. Watters (S'82–M'88) received the Ph.D. degree from Northwestern University in 1989. His research was in the field of electromagnetic thermal processing and characterization.

He is presently at SRI, Palo Alto, CA.

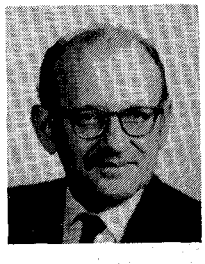

Morris E. Brodwin (A'49–M'55–SM'68–LS'90) received the Ph.D. degree from Johns Hopkins University in 1957. In addition to studies in applied and theoretical microwave communications and radar, his main field of research was in the application of ferrites to microwave problems.

In 1958, he joined the faculty of Northwestern University, where he is now Professor of Microwave Engineering in the Electrical Engineering and Computer Science Department. He has applied microwave techniques to study charge transport processes in semiconductors, magnetized semiconductors, and anisotropic gas plasmas. More recently, he has been using microwave characterization to study ionic transport in solid electrolytes. He is presently involved in the microwave characterization and thermal processing of ceramics and cements.

Dr. Brodwin has received the Service Award and the Outstanding Engineer Award of Region IV.